

MEASUREMENT OF DYNAMIC THRUST PRODUCED BY CAMAR UAV MODEL V1

MOHD NAJIB BIN AB RAZAK

UNIVERSITI TEKNOLOGI MALAYSIA

UNIVERSITI TEKNOLOGI MALAYSIA

DECLARATION OF THESIS / UNDERGRADUATE PROJECT PAPER AND COPYRIGHT

Author's full name : Mohd Najib Bin Ab Razak
 Date of birth : 02 September 1984
 Title : Measurement of Dynamic Thrust Produced By CAMAR UAV
 : Model V1

Academic Session : 2018/2019 Semester 1

I declare that this thesis is classified as:

- | | | |
|--------------------------|---------------------|---|
| <input type="checkbox"/> | CONFIDENTIAL | (Contains confidential information under the Official Secret Act 1972)* |
| <input type="checkbox"/> | RESTRICTED | (Contains restricted information as specified by the organization where research was done)* |
| <input type="checkbox"/> | OPEN ACCESS | I agree that my thesis to be published as online open access (full text) |

I acknowledged that Universiti Teknologi Malaysia reserves the right as follows:

1. The thesis is the property of Universiti Teknologi Malaysia.
2. The Library of Universiti Teknologi Malaysia has the right to make copies for the purpose of research only.
3. The Library has the right to make copies of the thesis for academic exchange.

Certified by:

SIGNATURE

SIGNATURE OF SUPERVISOR

840902015925
 (NEW IC NO. /PASSPORT NO.)

Dr. Ing Mohd Nazri Bin Mohd Nasir
 NAME OF SUPERVISOR

Date: 25 December 2018

Date: 25 December 2018

NOTES:

*

If the thesis is CONFIDENTIAL or RESTRICTED, please attach with the letter from the organization with period and reasons for confidentiality or restriction

I hereby declare that I have read through this thesis and in my opinion, it is sufficient in term of scope and quality for the purpose of awarding a Bachelor of Engineering (Mechanical)

Signature :
Name : Dr. Ing. Mohd Nazri Bin Mohd Nasir
Date : 25 DECEMBER 2018

MEASUREMENT OF DYNAMIC THRUST PRODUCED BY CAMAR UAV

MODEL V1

MOHD NAJIB BIN AB RAZAK

A project report submitted in partial fulfillment of the
requirement for the award of degree of
Mechanical Engineering

Universiti Teknologi Malaysia

25 DECEMBER 2018

DECLARATION

I declare that this thesis entitled “Measurement of dynamic thrust produced by CAMAR UAV model V1” is the result of my own research except as cited in the references. The thesis has not been accepted for any degree and is not concurrently submitted in candidature of any other degree.

Signature :

Name : Mohd Najib Bin Ab Razak

Date : 25 DECEMBER 2018

DEDICATION

To my lovely mother, who gave me endless love, trust, constant encouragement over the years, and for her prayers.

To my Family, for their patience, support, love, and for enduring the ups and downs during the completion of this thesis.

This thesis is dedicated to them.

ACKNOWLEDGEMENT

Alhamdulillah, praise to Allah S.W.T for giving me the strength to complete this thesis successfully.

I wish to express my most profound appreciation to all those who helped me, in one way or another, to complete this project. First and foremost I thank God almighty who provided me with strength, direction, and purpose throughout the project. Special thanks to my project supervisor Dr.-Ing. Mohd Nazri bin Mohd Nasir, CEng for all his patience, guidance and support during the execution of this project. Through his expert guidance, I was able to overcome all the obstacles that I encountered in these enduring four months of my project. He always gave me immense hope every time I consulted with him over problems relating to my project.

Special dedication to my wife Fauziah Binti Ismail, my son Muhammad Furqan and my family for her patience and sacrifices for all these years. Thanks a lot for the endless supports and inspirations given to me while completing this thesis.

ABSTRACT

Dynamic thrust is a Work done by a fan or a fan to deliver a forward motion. It is equivalent to the result of mass / second flows and the difference between slip velocity and plane speed. We need to study the effect of dynamic modeling using the appropriate procedures required to compare the impact of the model with the fan and without the fan. The results of this study will produce the coefficient of lift (CL), the coefficient of drag (CD) and coefficient of moment (CM) graphs. Graph CL vs. AOA (angle of attack) shows the maximum CL is at 8 degrees AOA (angle of attack) on both testing with propeller and without the propeller. However, the CD graph shows coefficient when using the propeller is slightly higher if compared with no propeller. Lastly, CM graph shows the value of the coefficient when no propeller is slightly higher if compared with when there is a propeller. I do this testing for the pitch angle -4° , 0° , 4° , 8° , 12° and 16° . While the other setting for yaw angle is 0° , 4° , 8° , 12° and 16° , yaw angle will set by the computer. Forces and moments sensed by the model were measured using JR3 Six Component Balance. This sensor is capable of returning three aerodynamic forces and moments, and it placed under the test section floor.

ABSTRAK

Pertama, kita perlu tahu bahawa tujahan dinamik adalah Kerja yang dilakukan oleh peminat atau kipas untuk menyampaikan gerakan ke hadapan. Ia bersamaan dengan hasil aliran besar / kedua dan perbezaan antara halaju slip dan kelajuan satah. Tujuan kajian ini adalah untuk mengukur kesan pemodelan dinamik dengan menggunakan prosedur yang sesuai untuk membandingkan impak model dengan peminat dan tanpa peminat. Hasil kajian ini akan dilihat dengan menghasilkan koefisien angkat (CL), pekali seret (CD) dan pekali momen (CM) graf. Grafik CL vs AOA (sudut serangan) menunjukkan CL maksimum ialah 8 darjah AOA (sudut serangan) pada kedua-dua ujian dengan kipas dan tanpa kipas. Walau bagaimanapun, graf CD menunjukkan pekali apabila menggunakan kipas sedikit lebih tinggi jika dibandingkan dengan tiada kipas. Akhir sekali, graf CM menunjukkan nilai pekali apabila tiada kipas sedikit lebih tinggi jika dibandingkan dengan apabila terdapat kipas. Saya melakukan ujian ini untuk sudut pitch -4° , 0° , 4° , 8° , 12° dan 16° . Sementara tetapan lain untuk sudut curang adalah 0° , 4° , 8° , 12° dan 16° . Sudut Yaw akan ditetapkan oleh komputer. Angkatan dan momen yang dirasakan oleh model diukur menggunakan JR3 Six Component Balance. Sensor ini mampu mengembalikan tiga daya dan momen aerodinamik dan diletakkan di bawah bahagian ujian.

TABLE OF CONTENT

CHAPTER	TITLE	PAGE
	DECLARATION	ii
	DEDICATION	iii
	ACKNOWLEDGEMENT	iv
	ABSTRACT	v
	ABSTRAK	vi
	TABLE OF CONTENT	vii
	LIST OF TABLES	x
	LIST OF FIGURES	xi
	LIST OF SYMBOLS	xiii
1.0	INTRODUCTION	
	1.1 Introduction to UAV	1
	1.2 Problem Statement	4
	1.3 Objective of study	5
	1.4 Scope of study	5
	1.5 Discussion of my research	6
2.0	LITERATURE REVIEW	
	2.1 Wind tunnel facilities	7
	2.2 wind tunnel model and its fabrication	10
	2.3 Propeller Characteristic and mechanism	12
	2.4 The position of the propulsion system at The tail of the fuselage.	15
	2.4.1 Nose mounting of the engine	16

	2.4.2	Central or central rear location	17
	2.4.3	Rear fuselage location	18
	2.4.4	Rear podded power plant	19
	2.4.5	Podded power plant located above Or below the fuselage	20
3.0		METHODOLOGY	
	3.1	Methodology Flow	21
	3.2	How to set speed for wind tunnel testing	22
	3.3	How to know motor and propeller size For model	23
	3.4	Blockage Ratio	24
	3.5	Estimation of Propeller Size	25
	3.6	How to Balance the propeller	27
	3.7	Equipment Used	27
	3.8	Description of components	28
	3.8.1	Motor Specification	28
	3.8.2	Motor Description	28
	3.8.3	ESC specification	30
	3.8.4	ESC Description	30
	3.8.5	Li-Po Battery specification	30
	3.8.5	Li-Po Battery Description	30
	3.8	Experimental Set up inside Wind Tunnel	31
4.0		RESULT AND DISCUSSION	33
	4.1	Graph coefficient of lift versus angle of attack	33
	4.2	Graph coefficient of drag versus angle of attack	35

4.3	Graph coefficient of moment versus angle of Attack	37
4.4	Yawing moment versus yaw angle	38
5.0	CONCLUSION	40
	REFERENCES	41
	APPENDICES	46

LIST OF TABLES

TABLE NO.	TITLE	PAGE
1	Characteristics and capabilities of UAVs present and discussed at the 2003 UAV workshop. (Source as adapted from: Shu and Gu (2006))	2
2	Motor Selection	27

LIST OF FIGURES

FIGURE NO.	TITLE	PAGE
2.1	Outlining differences in wind tunnel design. Courtesy of NASA	9
2.2	Colour-coded of an open-loop wind tunnel	9
2.3	CAD wind tunnel model. (Source as adapted from: Hemida and Krajnovic (2010)	12
2.4	Propeller terms	13
2.5	Nose powerplant – Scottish Aviation Bulldog Source as adapted from book Aircraft conceptual design synthesis by DENIS HOWE	16
2.6	Central engine – Bae Hawk Source as adapted from book Aircraft conceptual design synthesis by DENIS HOWE	16
2.7	Central engine –Bae (V/STOL) Source as adapted from book Aircraft conceptual design synthesis by DENIS HOWE	17
2.8	Rear fuselage located engine - Lockheed F 16 Source as adapted from book Aircraft conceptual design synthesis by DENIS HOWE	19
2.9	REaytheon hawker 800XP Source as adapted from book Aircraft conceptual design synthesis by DENIS HOWE	19
3.0	Graph to determine Model Air speed	22

3.1	Flow chart to determine model thrust	23
3.2	Flow chart to determine the motor and propeller size for model.	24
3.3	Graph for estimation of propeller size	26
3.4	Equipment flowchart	27
3.5	Block diagram for wire connection	28
3.6	UAV model experimental setup inside wind tunnel For testing.	31
3.7	Wind Tunnel Testing For Pitch Angle	32
3.8	Wind Tunnel Testing For Yaw Angle	32
4.1	Graph CL VS AOA	33
4.2	Graph Cl vs aoa (Source adapted from kumar et.al, 2015,5:2)	34
4.3	CD vs AOA	35
4.4	Drag curve for smooth NACA-018 air foil at two low Reynolds number (source adapted from JBbarloWH RaeJrAPope-low speedwindtunneltesting)	36
4.5	CM vs AOA	37
4.6	CM vs AOA for low Reynolds number	38
4.7	CL vs YAW ANGLE	38
4.8	Yawing moment vs sideslip angle (source adapted from effect of tail dihedral angle on lateral directional stability due to sideslip angle by amalina, suhaimi and wan Zaidi)	39

LIST OF SYMBOLS

T_c	=	Thrust coefficient
T	=	Thrust
ρ	=	density
V	=	Velocity
Q_c	=	torque coefficient
Q	=	torque
d	=	Diameter
n	=	rotation per second
V_s	=	velocity for full scale air plane
V_m	=	Velocity for model
d_m	=	Diameter model
d_s	=	Diameter for full scale air plane
T_{cm}	=	Thrust coefficient model
T_{cs}	=	Thrust coefficient for full scale air plane
C_{ts}	=	Thrust coefficient for full scale air plane
C_{tm}	=	Thrust coefficient for model
ESC	=	electronic speed controller
Re	=	Reynolds Number
L	=	length of tip chord
T_s	=	Thrust for full scale air plane
T_m	=	Thrust Model
μ	=	Dynamic viscosity
C	=	Chord

C_{yaw}	=	Coefficient of yaw moment
M_z	=	Moment in z direction
C_m	=	Coefficient of Moment
M_y	=	Moment in y direction
C_d	=	Coefficient of Drag
F_x	=	Force in x direction
C_l	=	Coefficient of lift
F_z	=	Force in z direction
N_s	=	Speed for Full Scale UAV
N_m	=	Speed for Model UAV
D_m	=	propeller model diameter
D_s	=	Diameter full scale propeller
V_m	=	Wind Tunnel Speed for Model UAV
V_s	=	Speed for full scale UAV

1.0 INTRODUCTION

1.1 Introduction to UAV

An unnamed aerial vehicle (UAV), commonly known as a drone, is an aircraft without a human pilot aboard (Technopedia, 2017). Unnamed aircraft system (UAS) is a recent development in the aviation field where it represents the cutting-edge and the advancement of technologies in the aerospace industry. The system itself constituted of a UAV, a ground based-controller and a system of communications. According to ICAO (2011), the flight of UAVs is built to be controlled by either remotely or autonomously through the onboard computers which makes it convenient and advanced. Due to this, UAV is capable of being used for various purposes, from military equipment to domestic surveillance (Technopedia, 2017). Although UAS received a controversial issue among citizens, researchers such as Gupta, Ghonge, and Jawandhiya (2013) emphasized the importance of UAS in many public and dangerous missions. The researchers also endorsed the integration of UAS into aviation system while at the same time, stressing on the need to consider its challenges and potential issues. Nonetheless, the integration and application of UAV is a ground-breaking invention which is worthy to be researched and improved.

By definition, UAVs are fully autonomous or semi-autonomous aircraft that carry cameras, communication equipment, sensors or another payload. In a research topic, discussions on UAVs have been around since the 1950s. The aircraft used in their prototype forms in World War I and II. In the past decades, numerous researches were initiated by the Defense Advanced Research Project Agency (DARPA) to increase the extent to which UAV adopted in military applications (Peter, 2009)). In recent years, numerous interests

have been coming from different federal, civilian and commercial applications, such as in the case of monitoring traffics.

By classification, UAVs are either fixed-wing or rotary-wing. The fixed-wing vehicles are easier to control, they have better endurance, and are the best when it comes to wide-area surveillance and application tracking. Another advantage of the fixed-wing vehicles is that they can be used to sense image from long distances. In any case, this form of vehicles also come with the disadvantage of taking significant time for the machines to react because colossal time and space required for turning a fixed-wing vehicle, which is mandatory until the vehicle regains its course. On the other hand, the rotary-wing vehicles known as Vertical Take-off and Landing (VTOL) vehicles (Shu and Gu, 2006). They come with the advantage of minimum launching time, and they don't need big space for landing. They also come with a higher level of hovering and maneuverability. Rotary-wing vehicles come with cameras and short-range radars for detecting movement of traffic. However, they have a disadvantage as the rotary motion results to vibration (Ota, 1983).

Table 1: characteristics and capabilities of UAVs present and discussed at the 2003 UAV workshop (Source as adapted from Shu and Gu (2006))

Vehicle	Endurance (hours)	Payload Weight (kg)	Altitude Capacity (ft)
Aerosonde	40	1	20,000
Altus2	24	150	65,000
AV Black Widow	5	0	1,000
AV Dragoneye	1	0.5	3,000
AV Pointer	1.5	0.9	3,000
AV Puma	4	0.9	3,000
AV Raven	1.25	0.2	3,000
BQM-34	1.25	214	60,000
Chiron	8	318	19,000
Darkstar	8	455	45,000
Exdrone	2.5	11	10,000
Global Hawk	42	891	65,000
Gnat 750	48	64	25,000
Helios	17+		97,000
MLB Bat	6	1.8	9,000
MLB Volcano	10	9	9,000
Pathfinder	16	40	70,000
Pioneer	5.5	34	12,000
RMAX	1	28	500
Predator	29	318	40,000+
Shadow 200	4	23	15,000
Shadow 600	14	45	17,000

Different UAVs come with different payload weight carrying capabilities, and there is a significant variation on their mission profile (regarding range, duration, attitude), their accommodation (regarding the environment, volume), and their data acquisition capabilities and command controls. It is as illustrated in the table (1) above.

1.2 Problem Statement

In recent days, there is a lot of research that has been done about designing the UAV model. Firstly to experiment with the UAV model, the propulsion system has come to attention. The propulsion system includes the motor used in the system and the propeller efficiency. A suitable motor needs to choose to give more efficiency to the system whereas propeller efficiency which consists of a number of the propeller, the size of the blade, the pitch and the diameter used on the propeller is also essential as these will affect the UAV performance. The selection of these two criteria is necessary to ensure the capability of the system to give a better UAV performance.

By using a motor to rotate the propeller, it will also produce a torque force which will turn the UAV in the opposite direction for the propeller. This torque force contributes an essential effect on the dynamics of the UAV. For example, multicopters often rely on varying the speed of their motors to produce a net torque that rotates the aircraft in the desired direction.

Also, propeller efficiency also affects UAV performance. One of the factors of an unbalanced propeller is the propeller produces excessive vibration. The vibration travels through the entire airframe affecting the handling of the UAV, hence, produces inaccurate readings by the sensors, and creates premature failure of motor bearings and parts.

The propulsion system consists of a motor, propeller, electronic speed controller, and an electric battery. Combination selection of motor and propeller plays an important aspect to ensure the capability of the UAV system. When we select the motor and propeller combination, it is essential to determine the specific application area to generate the twice flying weight of UAV. It is because both the motor and propeller combination produces thrust and moves the vehicle.

1.3 The objective of the study

- I. To design measurement techniques to remotely quantify dynamic thrust
- II. To measure the performance of the propulsion system powered by CAMAR UAV model.
- III. To measure the impact of the dynamic scaling of the model using the appropriate procedure

1.4 The scope of the study

- I. To do literature study on propulsion system V3 used in UTM UAV known as CAMAR V1.
- II. Need to experiment, and the experiment will be executed at wind speed 40m/s
- III. Will do other setting and nature of the experiment shall be relevant to CAMAR V1.

1.5 Research Discussion

As mentioned by previous researchers, the difficulties in developing and applying an optimal measurement method to quantify the dynamic thrust created by the propellers are apparent and concrete. Since the dynamic thrust directly influences the performance flight of a UAV, hence it is critical to measure the dynamic thrust beforehand. The challenges lie on how this force can be remotely quantified and how its propulsion performance can be measured simultaneously (Logen et al., 2005). A recent study by Rutkay and Laliberté (2016) in measuring the performance of propulsion system concluded that although the propeller performance can be improved over time, however, the potential issues are with the efficiency and the power consumption of UAVs. The researchers also emphasized the importance of ground and wind tunnel testing in producing the feasibility of producing propellers with desired performance. In 2015, a group of researchers in Universiti Teknologi Malaysia (UTM) had successfully developed a UAV through the Consolidated Advanced Model for Aeronautical Research (CAMAR) model. This prototype is used to execute various mission which includes aerial monitoring and terrain mapping (Hamzah, 2015). By using this prototype, this research hopes to measure its dynamic thrust performance via an appropriate measurement. In doing so, the finding of this study will be able to address the challenges on remotely quantify the dynamic thrust and provide some practical solutions for future references. Also, this study could also act and serve as a future reference on the performance of the propulsion system by CAMAR model which is currently few and limited. Moreover, this study would also provide some useful insight on the impact of dynamic scaling of the model using the designated procedures. It could be another breakthrough in the field of aerospace since measuring the effect of dynamic scaling of a new model can be both challenging and difficult (Abobaker, Petrović, Fotev, Toumi, & Ivanović, 2017). Hence, it is relevant and worthy to measure the dynamic thrust on CAMAR V1 developed by UTM.

2.0 LITERATURE REVIEW

2.1 Wind tunnel facilities

A wind tunnel testing is an essential tool used in aerodynamic research to study the effects of air through solid objects. The wind tunnel consists of a tube path with the object under the test mounted in the center. Air is made to move outside the object by a strong fan system or other means. Test objects, often referred to as wind tunnel models, and are equipped with sensors suitable for measuring aerodynamic strength, pressure distribution or other aerodynamic-related features. (Going with the flow, Aerospace Engineering & Manufacturing, March 2009, pp. 27-28)

A wind tunnel is a tool that allows researchers to travel through the air to simulate flight and analyze aerodynamic properties of flow, such as elevation and drag. The wind tunnel is designed to deliver continuous and continuous airflow to the test portion and minimize the turbulence. In his article, Stathopoulos (1984) described and explained the requirement needed to design and fabricate the wind tunnel. In his context, the wind tunnel is built to explore the aerodynamic characteristics of a plane or an aircraft. The researcher indicated that the geometry and flow characteristics of the wind tunnel had been based on the commercial and space availability consideration. Over the years, however, the designs of wind tunnel have drastically changed due to the advancement of technologies and the innovation developed by other researchers. This development will be discussed in the later section of this study.

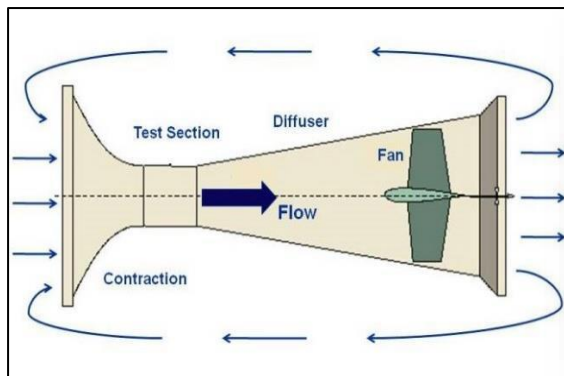
Wind tunnels are essential for aerodynamic studies. Since its inception in 1871. (National Aeronautics and Space Administrations, 2015), they have undergone some iterations regarding design; the two most common configurations it is an open circuit wind

tunnel and closed-circuit wind tunnel, shown below in Figure (2.1). Both have the same essential components, but the design and construction are generally different. Significantly. According to the previous researchers also, their design has also considerably influenced their overall purposes which in turn, can be differentiated based on their apparent differences and significant drawbacks.

An open circuit wind tunnel releases air from the environment and expels them to the atmosphere after leaving the fan, while the closed circuit wind tunnel generates circulating circuits with air circulating over the tunnel. The design of a closed circuit wind tunnel offers better efficiency and produces some noise, but it's more expensive and more difficult to produce. Challenging to manufacture. According to Mat Bahari (2012), the open-loop wind tunnel is one of the easiest ways to measure the aerodynamic characteristics. However, depending on the model tested, he further commented that the open-loop wind tunnel might not be the best approach to obtain an accurate and reliable result.

Meanwhile, Calautit, Chaudhry, Hughes, and Sim (2014) argued that although many types of research prefer open-looped wind tunnel due to its low power consumption, closed-loop wind tunnel proven that the outcome is much desirable. To support this claim, Kulkarni et al. (2012) relate the advantages of a closed circuit wind tunnel design with superior control over flow quality. Figure (2.2) illustrated the design of both the open-looped design wind tunnel and the closed-loop wind tunnel.

Open loop-design



Close loop-design

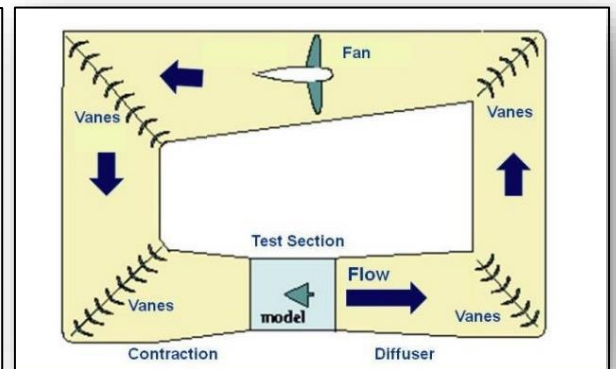


Figure 2.1: Outlining differences in wind tunnel design. Courtesy of NASA

An open-loop wind tunnel consists of 5 primary components, listed from left to right on **Figure (2.2)** below: a settling chamber, contraction section, test section, diffusing section, and a fan (National Aeronautics and Space Administrations, 2015).

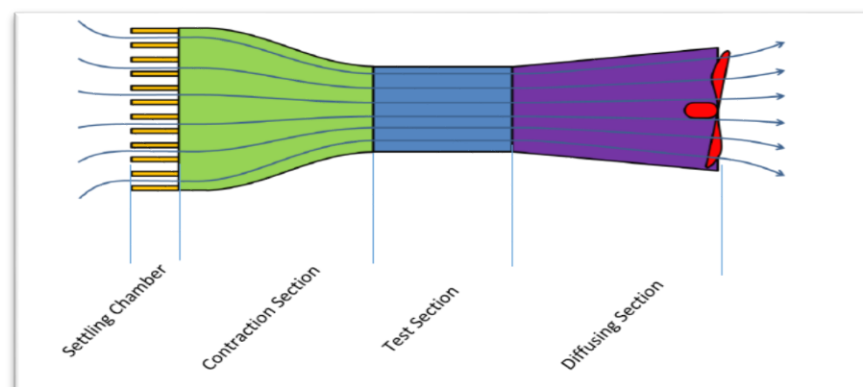


Figure 2.2: Colour-coded of an open-loop wind tunnel

A wind tunnel is an object that used in aerodynamic research to study the effects of air passing in front of a solid object. A wind tunnel has a tubular passage with the object under test mounted in the middle. Air is made to run past the purpose by a powerful fan system. The test object also called a wind tunnel model, is instrumented with suitable sensors to measure aerodynamic forces, pressure distribution, or other aerodynamic characteristics. Previous studies have used the wind tunnel test on UAVs to examine the

aerodynamic characteristics of a UAV. Experiments conducted by both Jindeog, Jangyeon, Bongzoo, and Samok (2003) and Moyer and Talbot (1994) have discovered that wind tunnel is capable of calibration and model verification and testing on UAVs. Both studies were able to explore and research the surface deflections, lift curve slope, pitching moment variation with lift coefficients and drag polar of a UAVs. Since both of the studies did not consider the power consumption in their construction expenditure, both concluded that the open-looped wind tunnel appears to be more feasible and flexible as compared to the closed-looped design. However, there are still some researchers that argue otherwise (Calautit, Chaudhry, Hughes, & Sim, 2014; Kulkarni et al., 2012).

2.2 Wind tunnel model and its fabrication

The wind tunnels were invented towards the end of the 19th century, in the early days of aeronautics research, when many attempted to develop successful heavier-than-air flying machines. The wind tunnel has been conceived as a way of reversing the conventional paradigm. Instead of standing still and letting the object pass at high speed, the same effect will be obtained if the goal remains motionless and the air passes full speed. In this way, motionless observers can learn flying objects in action and measure the aerodynamic forces imposed on them.

The development of wind tunnels accompanies the development of the aircraft. The Large wind tunnels were built during the Second World War. Wind tunnel tests are considered important in the development of aircraft and supersonic missiles by the Cold War. After that, the wind tunnel study became very important: the wind impact on human-made structures or objects need to be studied when the building is high enough to present a large surface to the wind, and the building's internal structure is forced to withstand the resulting power. Determine, such effects were required before building codes could specify the required strength of such buildings and such tests continue to you for large or extraordinary buildings.

However, then, wind tunnel testing is used for cars, not much to determine aerodynamic power, identify means to decrease the energy required to move the vehicle on the road at a certain speed. In this study, the interaction between road and vehicle plays an important role, and this interaction must take into account when interpreting test results. In the real situation, the road moves relative to the vehicle, but the air relies relatively on the vehicle on. The way on, but in the wind tunnel, the air is moving relative to the roadway, while the roadway is fixed compared to test vehicles. Some motor vehicle test booths have incorporated a moving belt to approximate the actual condition, and very similar devices you in wind tunnel testing of aircraft take-off and landing configurations. (Barlow, Pope, & Rae, 1999).

The test of wind tunnel sports equipment has also been widespread throughout the year, including golf clubs, golf balls, Olympic bobsleighs, Olympic bicyclists and racing car helmets. Aerodynamic helmets are essential in open cockpit racing cars (Indycar, Formula One). Excessive lifts on helmets can cause large tension on the driver's neck, while the separation of the trunk on the back of the helmet can cause blurred and blurred vision for drivers at high speed. (Racing Helmet Design, James C. Paul, P.E., Airflow Sciences Corporation, 1993).

The design of the wind tunnel model is based on tradeoff and a combination of many requirements like the cross-sectional areas economic and available wind tunnel. The real shape and size of the missile that will be evaluated, the exact performance (regarding speed) of the air vehicles, Reynolds number materials, the similarity of the loaded parameters and the production process of the model together with other things. A version of a model shown in the figure (2.3) below. This model is a scale at 1:7, featuring four body sections as nose section, section-II, balance section or mid-section, and wing and tail section. There is also wire tunnel in this model, and the tunnel divides into three parts, then attached at section II, III and IV to stimulate real-time flight situation. The section IV is

where the wings located at four orthogonal positions. The tail panels having zero control deflection can be attached with the wings.

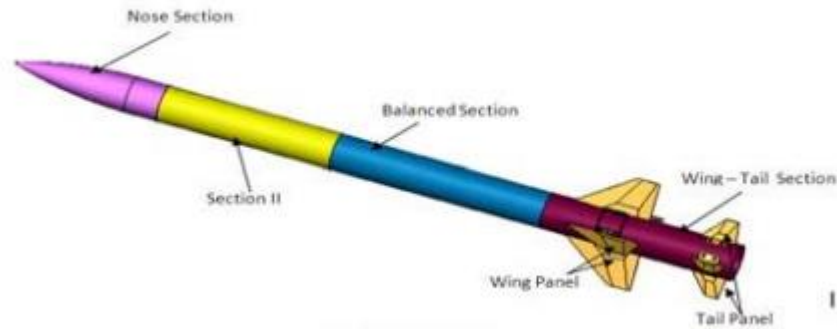


Figure 2.3: CAD wind tunnel model (Source as adapted from: Hemida and Krajnovic (2010))

2.3 Propeller Characteristic and mechanism

By definition, a propeller is a mechanical device used for propelling an aircraft or a boat, consisting of a moving shaft and two or more broad, angled blades are attaching to the shaft. Being initially invented for the radio controlled (RC) model aircraft, the propeller has become one of the common propulsion device used in UAVs. Rutkay and Laliberté (2016) explained that the rotary motion created by a propeller developed a different air pressure between front and back surfaces of its blades which then lead to lift or thrust but in the forwarding direction. Its geometry determines Propeller's performance, and different propeller geometries are optimized to produce thrust efficiently at given rotational and forward flight speeds. When the propeller rotates, the blade will push the air in one direction. because the propeller is pushing air in one way, the air also pushing the

propeller to way contrary to the same power. This power is known as a thrust and it's used to move the aircraft.

A propeller is typically characterized by two or more blades that are attached to a central hub with the hub mounted on an engine crankshaft, or in some cases to the output shaft of a reduction gearbox. Typically, a spinner is used to guide the center, and the spinner also plays the role of enhancing appearance and aerodynamics. The propeller is to convert engine power into a useful thrust that can be used to flight aircraft and keep them flying (Campso, 2008). The full components of a propeller are as illustrated in the figure (2.4) below.

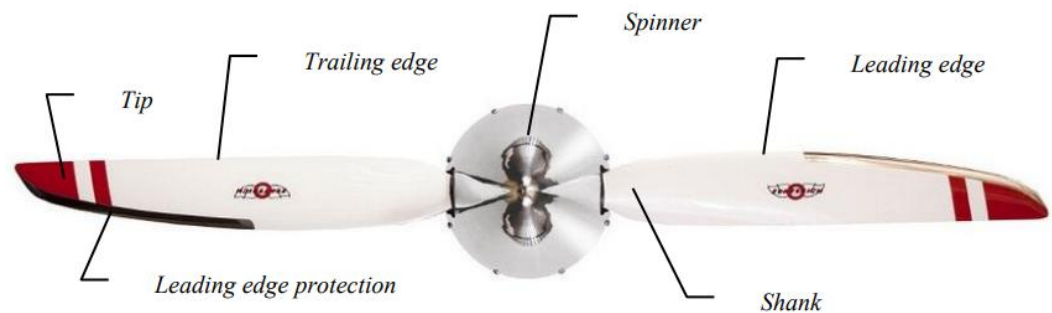


Figure (2.4): Propeller terms (Source as adapted from: Campso (2008))

Besides the components highlighted above, a propeller also has a control system. Modern propellers being used on large turboprop aircraft have up to 6 blades. Other parts of a propeller include a spinner that is used to create aerodynamic streaming over the hub of a propeller. A bulkhead provides room for the spinner to be attached to the propeller. The effect of the propeller model and motor simulation is an important part of wind tunnel testing in an airplane. Both the complexity and the importance of this simulation are because the aerodynamic phenomena linked to the propeller are very complex, which include complexity on the way the propeller interacts with the airframe (Pope et al. 1999). Most of the propellers have only two blades because a two-bladed propeller is more efficient than a larger propeller that will produce the same thrust and airspeed. Cannot use

single blade propeller because of dynamic unbalance. It also depends on the power coefficient because lower RPM give better propeller efficiency. As Rutkay and Laliberté (2016) mentioned in their research, the purpose of the propeller is to apply the mechanical energy into the thrust. Given that both motor and battery drive the propeller at peak efficiencies, the ideal design of a propeller is sometimes impossible an unrealistic to be achieved.

A multi-bladed propeller does not have more induced drag which is due to tip vortices. So, overall efficiency is lower. It also often has a larger total blade surface area than the equivalent larger two-bladed propeller, For the best performance and efficiency, reduced noise, and increased motor life, all propellers should be balanced before use. Multi-bladed propellers can turn power into thrust and airspeed in less space than a larger two-bladed propeller though, which makes them advantageous when ground clearance is an issue (or fuselage clearance for wing or pylon mounted propellers). (Günel & Ankaralı, 2016). As reported by Logan et al. (2005), achieving the optimal performance for the propeller is complicated, given that several factors such as poor methods of analyzing the aircraft's performance at low Reynolds numbers are difficult to be investigated and determined.

Dynamic thrust is the work done by the propeller or a fan to give forward motion, it is equal to the product of mass flow/second and the difference between slipstream velocity and aircraft speed. Wind tunnel experiments must be performed to analyse the aerodynamic properties of an unmanned-aerial-vehicle (UAV), or system identification can be made from experimental flights. Being able to predict the propeller thrust and rotor drag can help identify other aerodynamic properties of a UAV, such as the drag of the vehicle or the amount of lift a wing produces.

Propellers can be characterized into different types based on their systems. The fixed pitch propeller is one of them it is it is the most widely adopted design for propellers in aviation as a result of its simplicity. This form of propellers is common in light single-

engine aircraft. The second type is ground adjustable propeller which is similar to the fixed pitch propellers in the sense that it is not possible to change their blade in flight. In any case, there is a major difference, which is that these propellers are designed in such a way that the blade angles are possible to be changed while on the ground, which imply that the propeller can be adjusted to offer the desired features necessary for a given flight. Two position propellers are designed to allow pilots make a selection on one or two blade angle while in flight, which means that it is possible to use a low blade angle for take-off and a high blade angle for landing. It is somewhat like what is obtainable in the two-speed transmission in an automobile (Hemida and Krajnovic, 2010).

Controllable pitch propeller is another example, and it is designed to allow the pilot change blades into any angle of choices within the range covered by the propeller while in flight, ensuring that the pilot has more control over propellers during flight. There is also automatic pitch changing propeller which is designed to function independently of the pilot. As against being controlled by the pilot from the cockpit, this propeller automatically sets the blades to the most efficient angle as it reacts with the force the engine loads and airspeed generates. Finally, constant speed propellers are adopted in the majority of the medium and high-speed aircrafts available today. This propeller system is based on controllable propeller that allows the pilot to directly control the system by adjusting to a constant speed control unit, which is known as the governor. The propeller blade is then adjusted by the governor to maintain the speed of the engine or rotations per minute as set by the pilot on the governor (Hhemida, and Krajnovic, 2010).

2.4 The position of the propulsion system at the tail of the fuselage

In many designs, the powerplant system is located within or on the fuselage, and when this is the case, it requires primary consideration and may provide the starting point for the layout. The fuselage is considered the main body of an aircraft. It generally includes space for personnel, cargo, and control. In this case, in UAV, it provides space for control. There are various accessories which are attached to the fuselage, namely wings, stabilizers,

landing gears, and power plant. There are five basic fuselage-located powerplant arrangements may be identified:

2.4.1 Nose mounting of the engine,

Figure (2.5). This arrangement is appropriate to both piston- and turbine-driven propeller engines. The powerplant determines the geometry of the front fuselage, including influencing the cross-section but has little another effect on the rest of the fuselage layout. An exception to this generalization is when the exhaust gases from a nose-mounted turbine engine are passed rearward through the fuselage rather than being ejected locally, but this is unlikely to be necessary for a view of the relatively low exhaust gas temperature and velocity associated with this class of engine.



Figure 2.5: Nose powerplant – Scottish Aviation Bulldog (Source as adapted from book Aircraft conceptual design synthesis by DENIS HOWE)

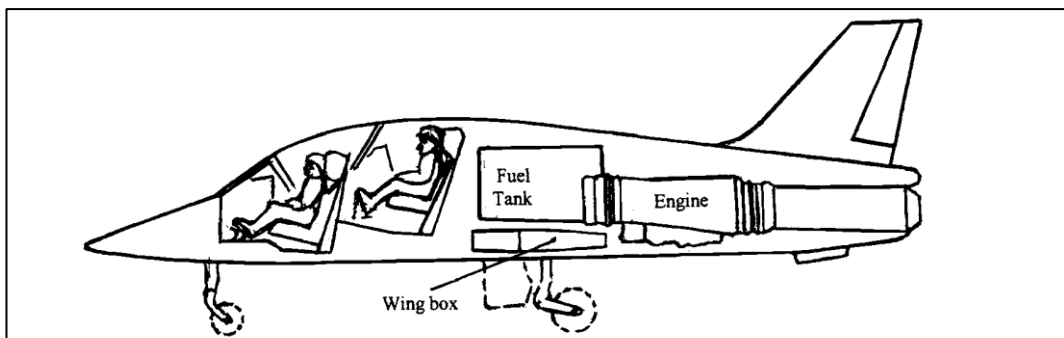


Figure 2.6: Central engine – Bae Hawk (Source as adapted from book Aircraft conceptual design synthesis by DENIS HOWE)

2.4.2 Central or central rear location.

Figure (2.6) and Figure (2.7) Show the location of the power plant system in the center of the fuselage can be advantageous in some circumstances, particularly for jet-powered military trainer/strike aircraft having wings of moderate aspect ratio. The positioning of the engine just aft of the main wing structure implies that its relatively high mass is near to the center of gravity of the aircraft. The intake system usually employs side or ventral fuselage intakes and may pass through the region of the wing center structure. A significant consideration is the means of engine removal. While there may be other possibilities, however, the best approach is to provide sufficient ground clearance for the engine to be removed downwards by removal of a lower surface access panel or through doors. It is also usually preferable for the exhaust gases to take out from the rear of the fuselage. The alternative of fuselage side exhausts is likely to give rise to acoustic fatigue problems at the back of the aircraft.

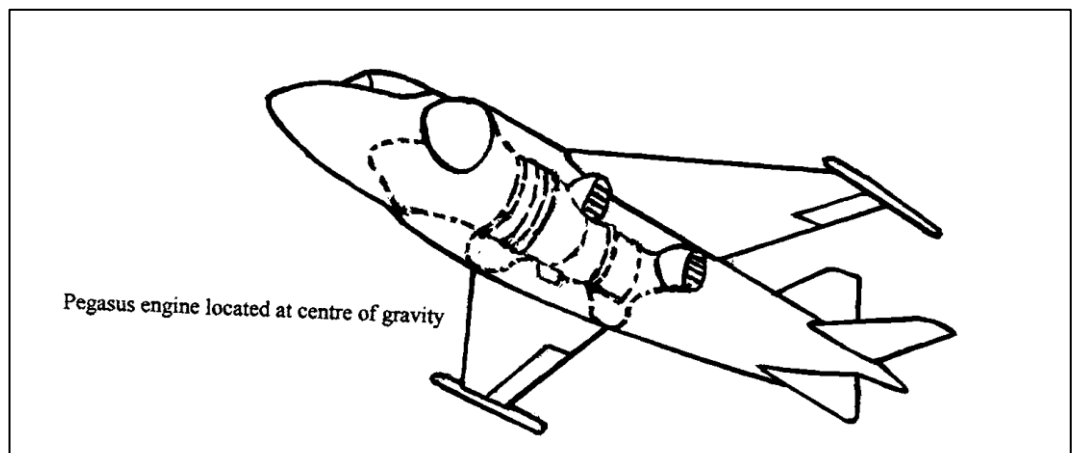


Figure 2.7: Central engine –Bae (V/STOL) (Source as adapted from book Aircraft

conceptual design synthesis by DENIS HOWE)

A particular case of a centrally mounted powerplant is that of a V/STOL aircraft, Figure 1.7 Regardless of the vertical lift system being used. It found that the main cruise/lift powerplant has to be fix at, or close to, the centre of gravity. As a result, the engine and centre wing structure occupy a similar fore and aft location in the fuselage. It

would appear that the position of the wing above the powerplant is the only practical solution, removal of the engine preferably being downwards. If one of the rationales for downwards engine removal is due to inadequate ground clearance, then the removal of the wing to enable engine withdrawal upwards may have to be considered as well. It is clear that when the engine is located in the centre fuselage the total powerplant system of the air intake, engine and jet pipes occupies a large part of the total fuselage volume and has a significant effect upon the overall layout.

2.4.3 Rear fuselage location,

Figure (2.8) shows the It is usual for the powerplant to fix at the rear of the fuselage in supersonic combat types which have wings of relatively low aspect ratio. An important advantage in this setting is that high-velocity exhaust gases are emitted aft of all primary structure without the need for a long exhaust pipe. It also means that because of the wide root chord the wing structure can pass round the fuselage forward of the powerplant, greatly facilitating engine removal. It is usually downwards or downward and aft. Against this, it is necessary to consider how to arrange the attachment structure for the empennage, but this difficulty lessened when the aircraft has a canard configuration. Occasionally there may be a requirement to locate the third engine in the rear fuselage of a transport aircraft, although this is less likely than was once the case due to improved engine reliability. Dorsal intakes are usually used, but side intakes are a possibility. The influence of the powerplant in this layout is limited to the rear of the fuselage.

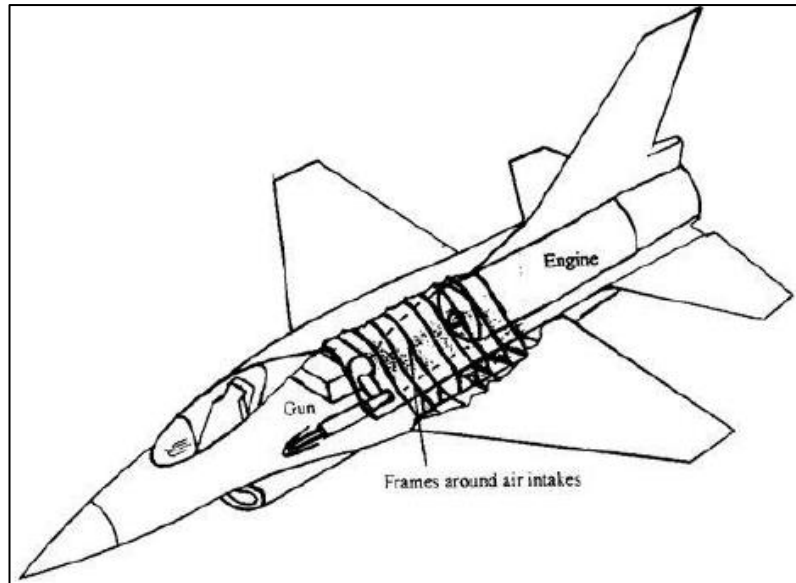


Figure 2.8: Rear fuselage located engine - Lockheed F 16 (Source as adapted from book Aircraft conceptual design synthesis by DENIS HOWE)

2.4.4 Rear podded powerplant

(Figure 2.9) Is the arrangement has only a secondary effect upon the fuselage layout. It is mainly restricted to the need to provide internal supporting structure and to avoid the location of flight critical components in the fan/compressor/turbine burst zones.



Figure 2.9: REaytheon hawker 800XP (Source as adapted from book Aircraft conceptual design synthesis by DENIS HOWE)

2.4.5 Podded powerplant located above or below the fuselage

The design of a fuselage is based on the aerodynamics, payload requirement, and structure of the UAV. The drag is affected by the overall dimension of the fuselage from numerous angles. By Hemida and Krajnovic (2010), a fuselage that has smaller fineness ratio do have fewer areas wetted for enclosing a given volume, but the area is more wetted if the length and diameter of the cabin are fixed. Improved aerodynamics for longer flights is created by higher Reynolds number and increased tail length, but this also results in the thin fuselage, generally at the expense of the structural weight. In the course of selecting the best layout, it is required that these trade-offs be studied in detail, however, before the engine process can be started, something must be chosen. Usually, this is done by selecting a value that is not far from existing aircraft that have a similar requirement, for which a much detailed study has been done. If such guidance doesn't exist, then, the choice should be to select an initial layout that meets the requirement for the payload

3.0 CHAPTER 3

METHODOLOGY

3.1 Methodology flow

Firstly, to start the experiment, we need to calculate the airspeed to be used for wind tunnel testing. Second, we need to experiment to find the required thrust for UAV Model. From that, we will calculate the propeller size for the third step. After we know the propeller size, we need to do a few experiments to find a suitable motor.

After we know the motor size, we will fix the motor and propeller to the UAV Model. Finally, we do testing inside a wind tunnel to take reading for force and moment. After we get the data, we will analyze to come out with the graph coefficient of lift, coefficient of drag, coefficient of pitching moment and coefficient of the yawing moment.

3.2 How to set speed for wind tunnel testing

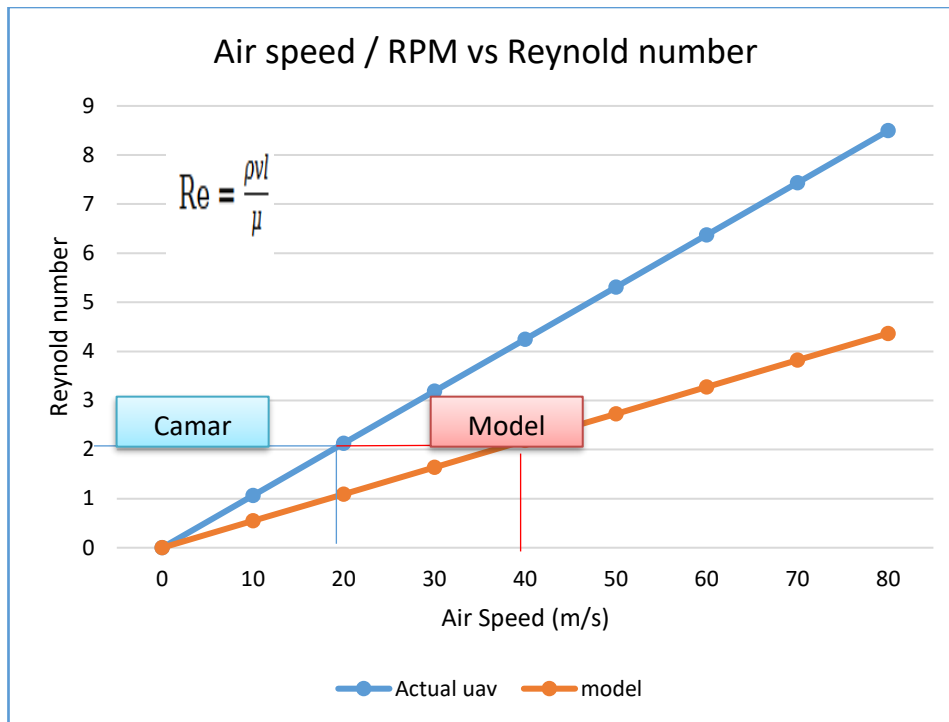


Figure 3.0: Graph to determine model air speed

By using the Reynolds number calculation and we use the different length of tip chord for CAMAR and MODEL. The variable value here is airspeed which is we change from 10m/s to 80m/s. After complete do the calculation, we will get a graph as above.

From that graph (blue colour) we already know the cruising airspeed for CAMAR, and from there we do a horizontal line to see the Reynolds number. Then from that Reynolds number we will draw a straight line to know the cruising speed for MODEL. From that graph, we know that the cruising time for MODEL is 40m/s.

Below is the Reynolds number formula for this calculation

$$Re = \frac{\rho v l}{\mu} \quad (1)$$

3.3 How to know the Motor and propeller size for UAV model

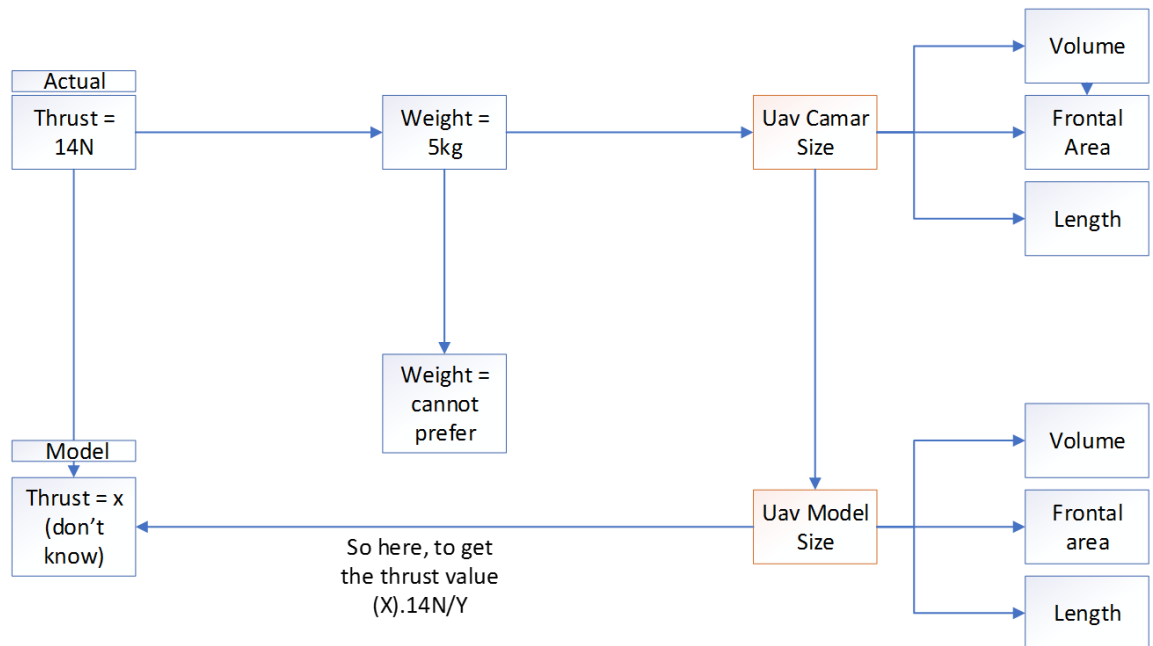


Figure 3.1: flow chart to determine the model thrust

From the above flowchart, we need to find the thrust value for MODEL. So we need to make a comparison until we know the UAV MODEL thrust value. Firstly we need to compare with the weight; we understand that the CAMAR model only 5kg but the MODEL weight is about 7kg because the UAV MODEL is made by fibre and CAMAR is made by Styrofoam and fibre, so the weight is not same. We cannot use to find the MODEL thrust.

The second option, we have to use CAMAR size and MODEL size and found that the size is scaled down is about 1:5 ratio (refer to the above graph for Reynolds number). So we can find the thrust by using the reduction factor. Reduction factor here is length, frontal area, and volume. After we get the reduction factor, we need to divide the CAMAR thrust with that reduction factor. So we know the MODEL thrust value.

After we know the thrust value, we need to do a lot of experiment to match the motor and propeller. Below is the flowchart to find the best motor and propeller.



Figure 3.2: flow chart to determine the motor and propeller size for model

From the above chart, we will test the motor only for 50% of throttle because we assume that 50% of throttle is the time for MODEL cruising time. We will do a few experiments until we get the best motor and propeller to use for testing inside the UTM closed loop low-speed wind tunnel.

3.4 Blockage Ratio

The blockage ratio is the ratio of frontal/projected/cross-section area (2D area seen from the front view) upon the cross-section area of the test section.

Blockage Ratio = Frontal Area of Model / Cross-section area of the test section (2)

Generally, a blockage of less than 5% should be preferred (Blockage effects are less). But for blockage more than 5%, blockage correction should be done to get good/valid results from experiments.

For this experiment already calculated the blockage ratio is 0.2230%. So the blockage is less than 5%.

3.5 Estimation of model propeller size for wind tunnel testing

Using advance ratio formula, we can calculate to estimate the model propeller size which will be used for wind tunnel testing.

Advance Ratio Formula:

$$\frac{V_s}{n_s d_s} = \frac{V_m}{n_m d_m} \quad (3)$$

N _m	rotational speed in rps (rotation per second)
V _m	wind tunnel speed model (refer sheet 1)40m/s
N _s	4700 rpm change to rps (78.33rps)
D _s	Diameter full scale propeller (13 inch)
V _s	speed full-scale airplane (22sm/s)
D _m	diameter propeller in (inch)

From this formula, we can calculate the size of the propeller. Below is the graph to show the propeller size to be used for wind tunnel testing.

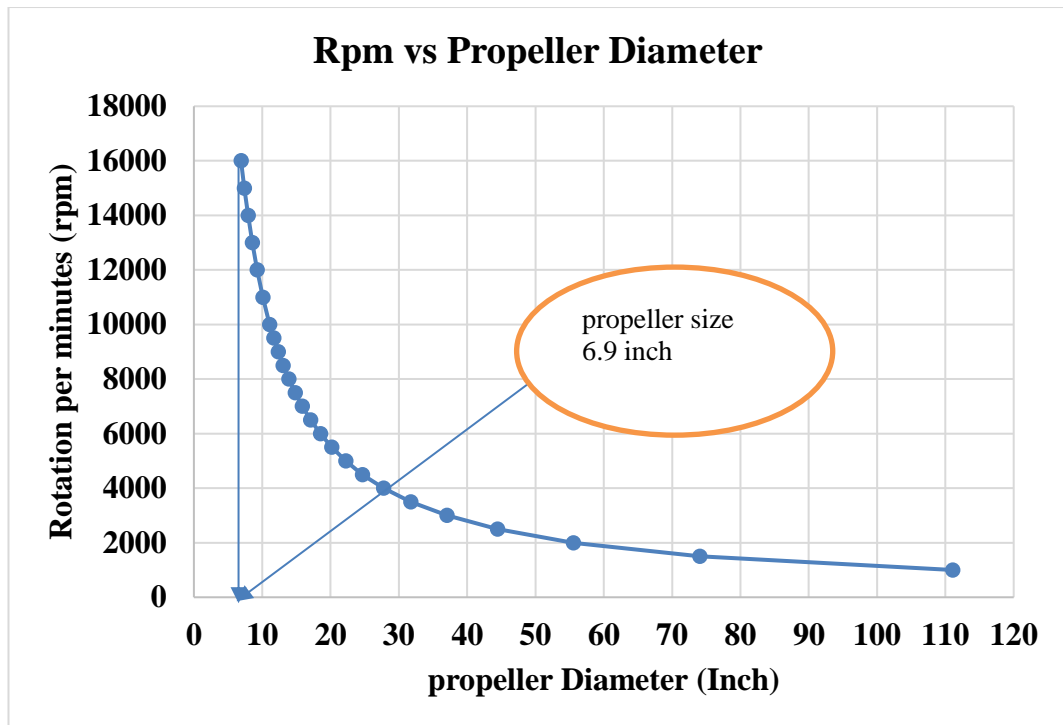


Figure 3.3: Graph for estimation of propeller size

From this graph, show that the propeller size to be used for wind tunnel testing is 6 inch, and we need brushless DC motor speed till 16000 rpm. For motor selection, we need to do a few an experiment to find a suitable motor for this propeller. Below is the testing to find the best motor.

Table 2: experimental to find a suitable motor for required propeller

Motor GT2826/04	
Propeller 8 x 5	9500RPM
	13.4A(11.1V)
Propeller 6 x 4	11000RPM
	5.5A (11.1V)
Propeller 6 x 4	15600RPM

	10.8A(14.8V)
--	---------------------

From this table (experiment), we know that we will use motor GT2826/04 with propeller size 6 x 4 for wind tunnel testing.

3.6 How the propeller will be balanced

Before final balancing, the propeller will be horizontally and vertically balanced. For horizontal balancing, the propeller's blade will be aligned horizontally along the balancer shaft. Plastics will be removed from the blade until the propeller stays propeller aligned in the horizontal position. For vertical balancing, the propeller will be vertically aligned along the balancer shaft. Once vertical balancing is done, the propeller will be turned back to the horizontal position to ensure that the propeller still maintains the horizontal balance. The propeller will continually be rotated between the vertical and horizontal position to ensure that removing material brings about improved balance. Finally, once the horizontal and vertical balancing is successful, the propeller will be turned to the angles along the balancer shaft (Richard, 2011).

3.7 Equipment used

Below are the Flowchart and block diagram for equipment used.

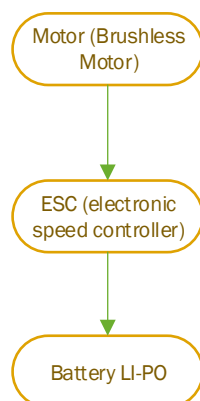


Figure 3.4: equipment flowchart

Block diagram (how to connect wire)

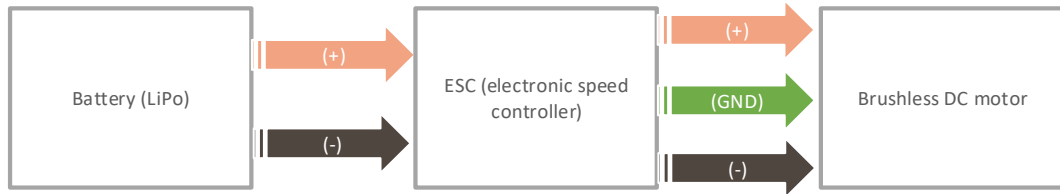


Figure 3.5: Block Diagram for wire connection

Before to perform an experimental setup, need to identify the equipment and components required. The component need is as below.

- a. Motor
- b. Esc (electronic speed controller)
- c. Li-Po battery

3.8 DESCRIPTION OF COMPONENTS

3.8.1 Motor specification

- Brand: Grand turbo
- Model: GT2826/04
- Propeller size to be fixed in the motor: 6 inch x 4inch
- Power rating: 11.1V to 14.8V
- Made by Emax

3.8.2 Motor description

Brushless DC motor can be explained as an electronically commuted motor which doesn't have brushes. This motor very efficient in producing a large amount of torque over a speed range.

Advantages of Brushless DC Motor

- The BLDC motor is more efficient as its velocity is determined by the frequency at which the current is supplied, not the voltage.
- Due to the absence of the brush, the loss of mechanical energy due to friction is less that increases the efficiency.
- BLDC motors can operate at high speed under any circumstances.
- No noise and noise less during operation.
- More electromagnetic can be used on the stator for more precise control.
- BLDC motors are very easy to accelerate and decelerate because they have low rotor inertia.
- It is a high-performance motor that provides large torque per cubic inch on a wide round.
- The Brushless DC motor doesn't have a brush that makes it more reliable, high expectations, and maintenance-free operation.
- There is no ionic splash of the commutator, and electromagnetic interference can also be reduced.
- A motor like this is cooled by conduction, and no airflow is required for cooling in it.

Disadvantages of Brushless DC Motors

- BLDC motor costs more than motor without DC brushless.
- Limited high power can be supplied to BLDC motor. If not too much heat weakens the magnet and the winding insulation may be damaged.

3.8.3 ESC specification

- Brand: Budget
- Current rated: 30A
- BEC: 2A/5v

3.8.4 ESC description

Electronic speed control or ESC is an electronic circuit with the aim of changing servo-motor speed, its direction and may also act as a dynamic brake. ESC is often used on motors providing three-phase electricity generated by low energy for the motor. It also allows for a finer and more accurate motor speed variation in a much more efficient way than the mechanical type with resistance coils and moving arms once used together. ESC can be a separate unit transmitted to the receiver throttle control channel or included in the receiver itself, as happens in most R / C toy class vehicles.

3.8.5 Li-Po battery specification

- Battery Capacity = 5000mAh=3Amp/hour
- Voltage = 14.8V
- Min Discharge rate 20C continuous
- Max discharge rate = 25C maximum

3.8.6 Li-Po battery description

The lithium-polymer battery (Li-Po, LIP or Li-Poly) is a rechargeable battery type that uses a soft polymer casing so that the lithium-ion batteries are located on a soft "outer pocket." It can also refer to lithium-ion batteries using gelled polymers as electrolytes. However, this term usually refers to the type of lithium-ion battery in the pocket format.

3.9 Experimental Setup inside Wind Tunnel

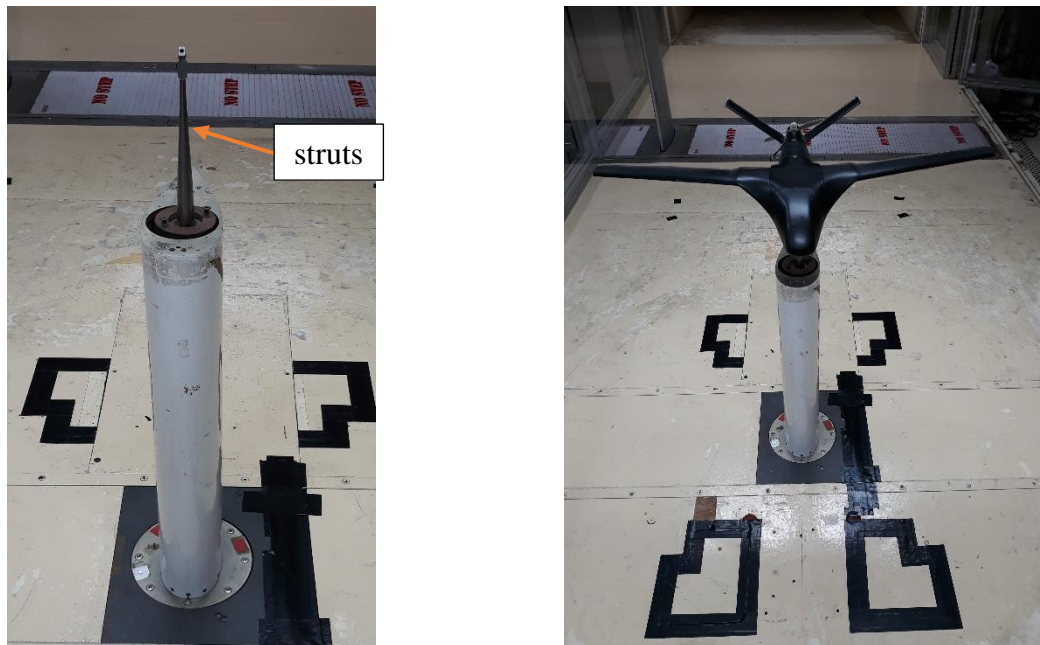


Figure 3.6: UAV model experimental setup inside wind tunnel for testing

Wind Tunnel Testing (WT) The static wind tunnel tests were conducted in the 1.5 m × 2 m × 5.8 m closed circuit Universiti Teknologi Malaysia Low-Speed Tunnel (UTM-LST). This facility is capable of providing maximum wind speed of 80 m/s with maximum turbulence intensity approximately 0.01 % across the test section. The model was mounted on single strut support while the model angle of attack was fixed to zero degrees. Forces and moments sensed by the model were measured using JR3 Six Component Balance. This sensor is capable of returning three aerodynamic forces and moments, and it is placed under the test section floor. The Balance Moment Center (BMC) is located at the center of this sensor. The sideslip angles were changed by rotating the tunnel, and all data have been corrected for tares caused by model strut support.

This experiment will include the test for:

- a. To test the different pitch angles (-4° , 0° , 4° , 8° , 12° and 16°).



Figure 3.7: wind tunnel testing for pitch angle

- b. To test the different yaw angles (0° , 4° , 8° , 12° , and 16°)



Figure 3.8: Wind tunnel testing for yaw angle

All above experiment will be done inside UTM (University Technology Malaysia) low speed wind tunnel.

4.0 CHAPTER 4

RESULTS AND DISCUSSIONS

4.1 GRAPH COEFFICIENT OF LIFT VERSUS ANGLE OF ATTACK

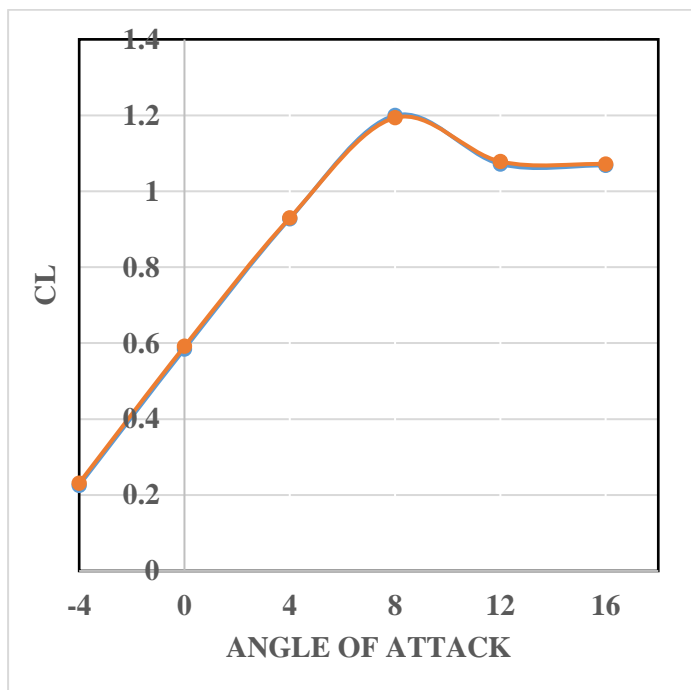


Figure 4.1: graph CL vs AOA

Figure 4.0.1 shows the two testing that has been done inside the wind tunnel. The red color was tested with the motor running at 15600 rpm, and the blue color was tested without the motor running. The results of this experiment show the starting coefficient of lift value at -40 angles of attack (aoa) is 0.07278. The highest amount of CL at 80 AOA.

The testing run inside the low-speed wind tunnel (UTM) with the airspeed 40m/s took one and half hours to complete.

From the figure 4.0.2, we can see the graph slightly different from figure 4.0.1. The lift coefficient (CL) varies significantly, steadily increasing until the stall occurs. (Kumar et al., J Aeronaut Aerospace Eng. 2016, 5:2). At the high angle of attack, it will cause the UAV loss to lift.

The coefficient of lift formula to generate the above graph is:

$$Cl = \frac{Fz}{0.5\rho v^2 C} \quad (4)$$

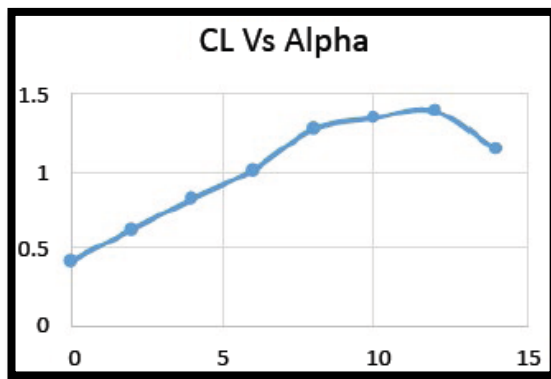


Figure 4.2: CL Vs AOA (source adapted from Kumar et al., J Aeronaut Aerospace Eng. 2016, 5:2)

4.2 Graph coefficient of drag vs angle of attack (aoa)

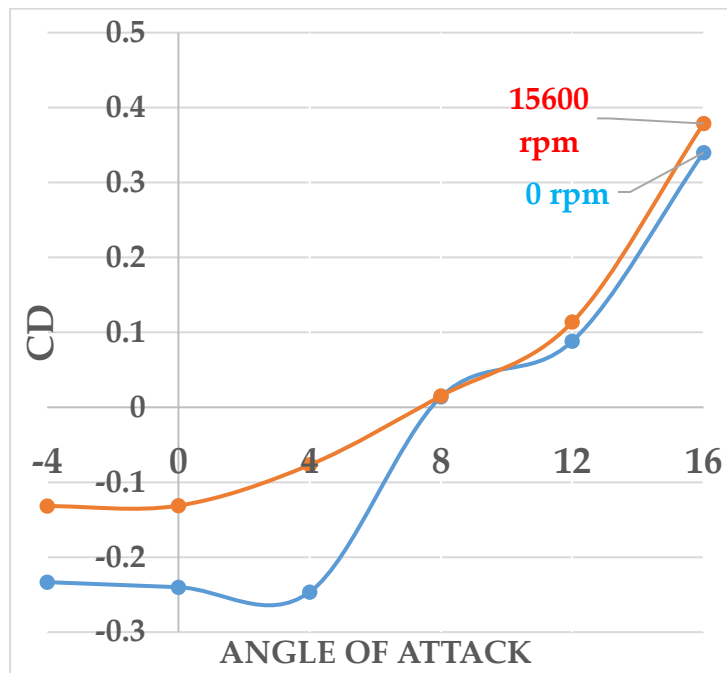


Figure 4.3: CD VS AOA

Figure 4.0.3 shows the cd vs. aoa. The red color line is testing with a motor (15600 rpm) and blue color testing without a motor as expected the drag increases with increase in AoA. Both experiment values increase exponentially with increasing AoA. When the motor is run at 15600 rpm, the lowest CD is -0.23329121. While the highest CD is 0.378698661, while the testing without the motor running, the lowest CD at -0.131843591 and the most top CD at 0.339953444.

At low angles, the drag is nearly constant and if the angle increase, drag will also increasing. The drag coefficient contains not only the complex dependencies of object shape and inclination but also the effects of air viscosity (James E. Brunk, 2015)

From the figure 4.0.4, we can see graph slightly different with diagram 4.0.3. Mueller and co-workers" give results of extensive studies of flow over two-dimensional airfoils at Reynolds numbers as low as 40,000 based on the chord. We show data for Reynolds numbers of 130,000 and 400,000 in Figures 17.2 and 17.3. At RN = 40,000 the lift curve for a NACA 663-018 from negative to positive stall is in three distinct pieces.

Two parts are near the stall, and at $\alpha = 8^\circ$, there is a linear region with a shallow slope (Kumar et al., 2016)

The coefficient of lift formula to generate the below graph is:

$$C_d = \frac{F_x}{0.5\rho v^2 c} \quad (5)$$

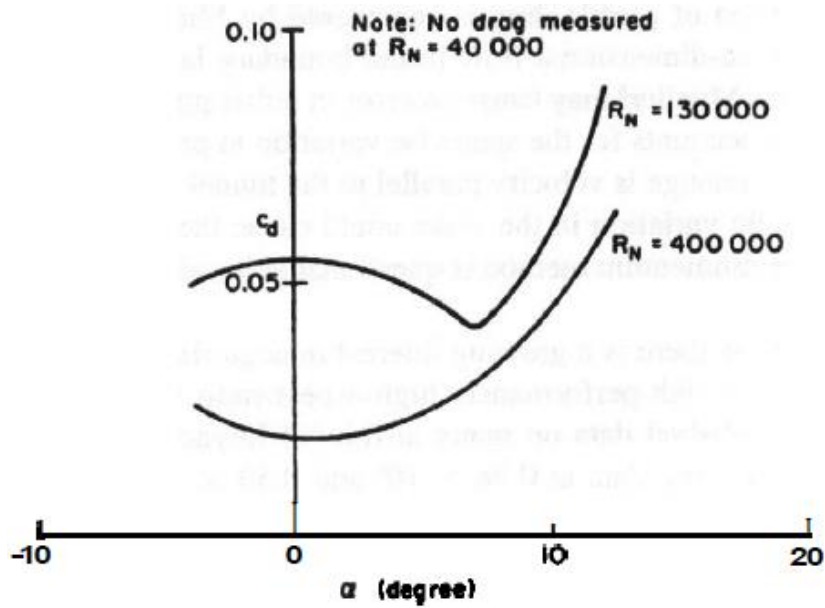


Figure 4.4: Drag curves for a smooth NACA 66-018 airfoil at two low Reynolds numbers. (Source from J.B.Barlow.H.RaeJrApope-LowSpeedWindTunnelTesting, 1999.)

4.3 Graph coefficient of pitching moment vs angle of attack (AOA)

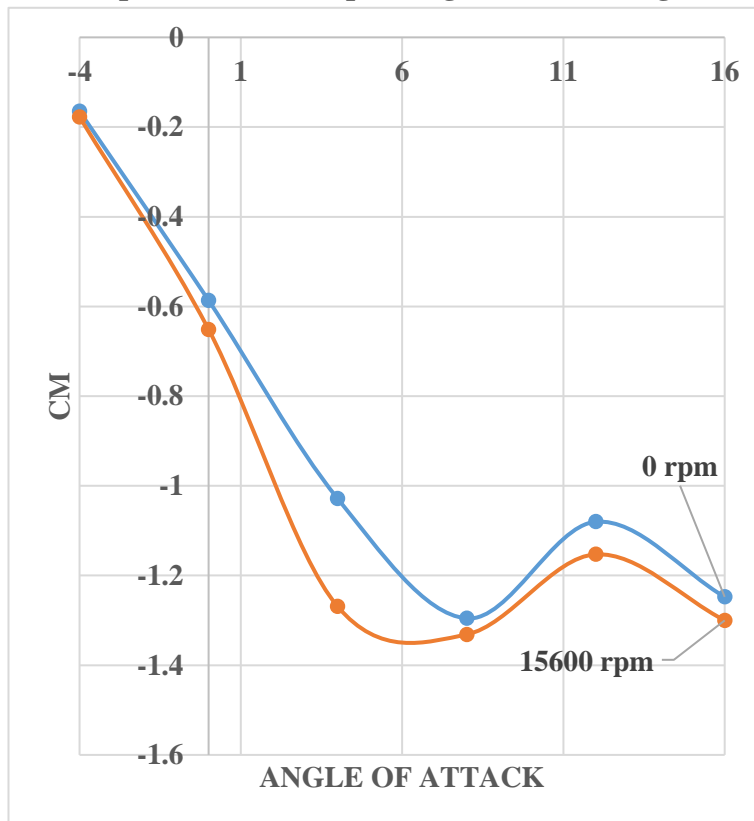


Figure 4.5: CM VS AOA

The coefficient of pitching moment formula to generate the above graph is:

$$C_m = \frac{M_y}{0.5 \rho v^2 c^2} \quad (6)$$

Figure 4.0.5 show CM vs. AOA. The orange color is testing with a motor (15600 rpm) and blue color testing without a motor. The highest CM for 15600 rpm is at -0.177487775 and the lowest coefficient at -1.30004. We may conclude that value CM without motor running is slightly higher than testing with the motor.

From the figure 4.0.5, we can see the graph decrease and the same scenario occur with the figure 4.0.6 which the graph decreasing as well. The chart show that the negative slope for positive α indicates stability in pitching due to low Reynolds number (Ira H. Abbott, and Albert E. Von Doenhoff (1959)).

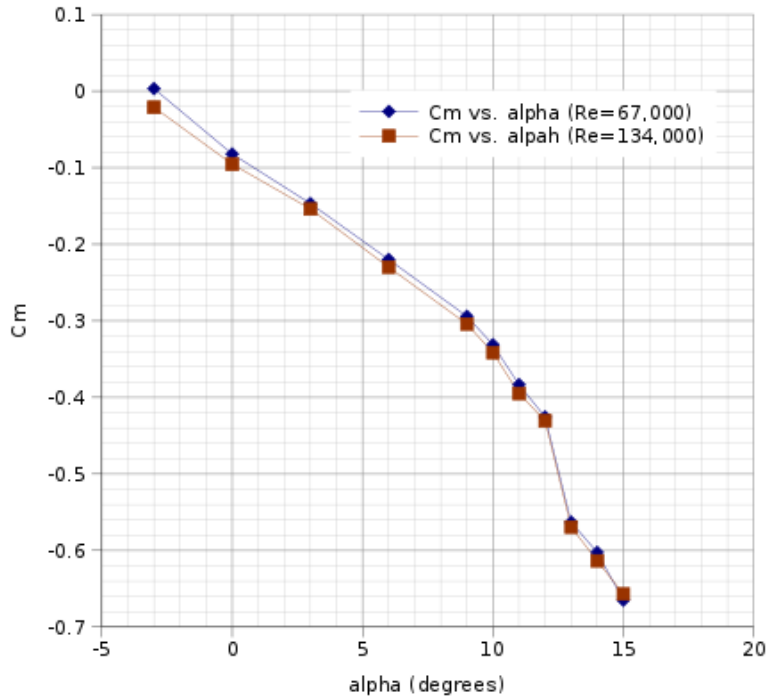


Figure 4.6: CM vs AOA for low Reynolds number

4.4 Graph coefficient of yawing moment vs yaw angle

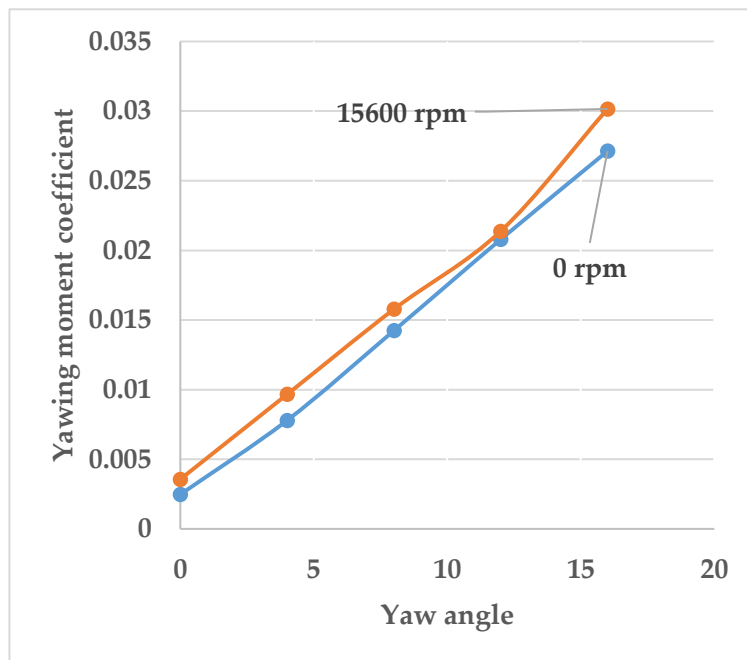


Figure 4.7: Yawing Moment Vs Yaw Angle

Coefficient of yawing moment formula to generate the above graph is:

$$C_{yaw} = \frac{M_z}{0.5\rho v^2 c^2} \quad (7)$$

From the figure 4.0.6 show yawing moment vs. yaw angle. The positive yaw angle generates a positive moment while negative yaw angle generates a negative moment. The highest yawing moment at 0.03 (using motor) and 0.0255 (without motor). This graph to show that the yaw moment about the z-axis and it is positive if he moves the nose of the plane to the right. The significant contributor to the yaw moment is the vertical tail.

If we compare the figure 4.0.6 with figure 4.0.7, V-Tail contributes to strong directional stability. Beside that v-tail also generates a higher rolling moment and this will lead to the cross-coupling problem with aircraft. (nur amalina, and suhaimi, 2009).

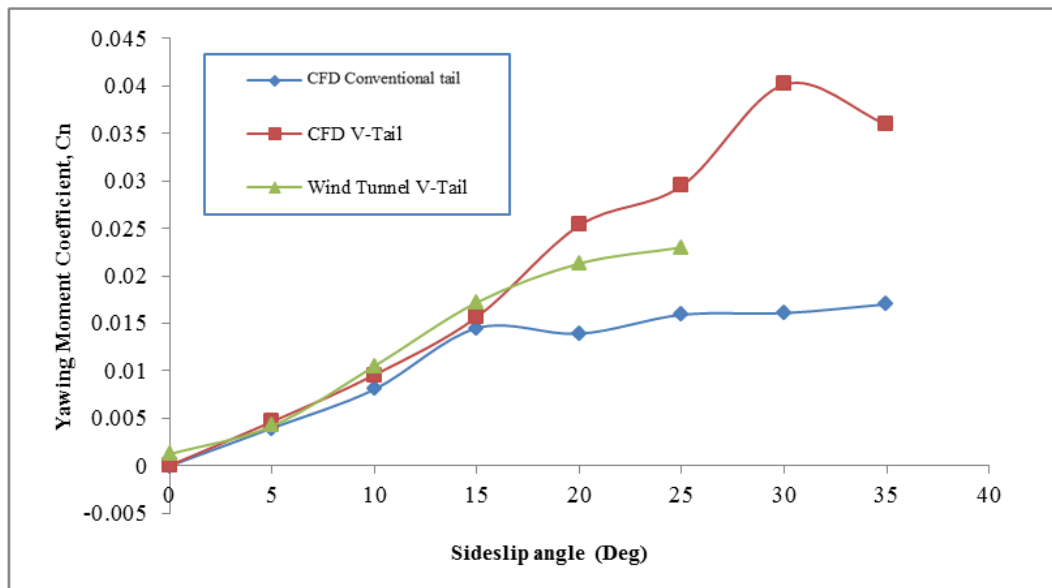


Figure 4.8: yawing moment vs sideslip angle (source from effect of tail dihedral angle on lateral directional stability due to sideslip angle by nur amalina, and suhaimi, 2015)

5.0 CONCLUSION

This research works and shows a good result for the coefficient of lift graph which the data found from testing with and without motor does not have much different. To quantify dynamic thrust, the testing run at the outside of wind tunnel due to know the required thrust so that from essential thrust it is easier to identify the correct BLDC motor that need to be used for wind tunnel testing. After run few testing, the required BLDC motor speed to get 6.2237 N thrust is at 15,600 rpm was obtained.

When the motor running by 15600 rpm at wind tunnel speed 40m/s, found that watt meter show the ampere at 0 (zero). It shows that the motor does not need much power to turn the propeller. The wind tunnel speed helps this to happened.

As a conclusion, there are not much different towards the coefficient of lift, the coefficient of drag and coefficient of the moment if we run with and without motor during wind tunnel testing. The scenario presented from the plotted graph. From lift graph, only 2.17% lift coefficient different while testing with and without a motor.

REFERENCES

- Abobaker, M., Petrović, Z., Fotev, V., Toumi, N., & Ivanović, I. (2017).
AERODYNAMIC CHARACTERISTICS OF LOW REYNOLDS NUMBER
AIRFOILS. Retrieved from DOI: 10.17559/TV-20160225100019
- Barlow, J. B., Pope, A., & Rae, W. H. (1999). *Low-speed wind tunnel testing*. New
York: Wiley.
- Calautit, J. K., Chaudhry, H. N., Hughes, B. R., & Sim, L. F. (2014). A validated design
methodology for a closed-loop subsonic wind tunnel. *Journal of Wind
Engineering and Industrial Aerodynamics*, 125, 180-194.
doi:10.1016/j.jweia.2013.12.010
- Campo, E., A. (2008), “Polymeric Materials and Properties”, William Andrew
Publishing, ISBN-13: 9780815515517, 249 pp.
- Choi, J.K., (2000) “Vortical inflow – propeller interaction using an unsteady three-
dimensional Euler solver’, Ph.D. Dissertation, The University of Texas at Austin
- Cui, D. (2008). “Structure technology development of large commercial aircraft”, Press
of Chinese Journal of Aeronautics, China, *Acta Aeronautica et Astronautica
Sinica*, v 29, n 3, 573-82, 25
- Fernández, E. G. (2010). Management System for Unmanned Aircraft System.
Aerospace Science and Technology.

- Günel, O., & Ankarali, A. (2016). Modeling of Basic Propeller Thrust Test System and Thrust Control Using PID method. *4th International Symposium on Innovative Technologies in Engineering and Science*.
- Hamzah, H. (2015, January 19). UTM Launched UAV CAMAR 1 Prototype. Retrieved from <https://news.utm.my/2015/01/utm-launched-uav-camar-1-prototype/>
- Hemida, H., and Krajnovic, S. (2010), “LES study of the influence of the nose shape and yaw angles on flow structures around trains”, Elsevier, *Journal of Wind Engineering and Industrial Aerodynamics*, v 98, n 1, p 34-46
- Huang, T.T. and Groves, N.C. (1980), “Effective wake: theory and experiment” 13th Symposium on Naval Hydrodynamics, Tokyo, Japan, 6-10 Oct. 1980.
- ICAO. (2011). *Unmanned Aircraft Systems (UAS)*. Retrieved from International Civil Aviation Organization website:
https://www.icao.int/Meetings/UAS/Documents/Circular%20328_en.pdf
- Jindeog, C., Jangyeon, L., Bongzoo, S., & Samok, K. (2003). Wind tunnel test of an unmanned aerial vehicle (UAV). *KSME International Journal*, 17(5), 776-783.
doi:10.1007/bf02983873
- Kulkarni, S., Minor, M., Deaver, M., Pardyjack, E., & Hollerbach, J. (2012). Design, sensing, and control of a scaled wind tunnel for atmospheric display. *IEEE/ASME Trans Mechatron*, 17(4), 635-645.
- Lattanzi, B. (2003). Dall'elica bipala di legno alla dodecapala composita a freccia; IBN Editore, Roma, (in italian).

Mat Bahari, M. A. (2012). DESIGN, CONSTRUCTION, AND TESTING OF AN OPEN-LOOP LOW SPEED WIND TUNNEL. *Unpublished thesis*.

Meirovitch, L. (2001). Fundamentals of Vibrations. McGraw-Hill International Edition.

Moyer, S. A., & Talbot, M. D. (1994). Wind-tunnel test techniques for unmanned aerial vehicle separation investigations. *Journal of Aircraft*, 31(3), 585-590.
doi:10.2514/3.46534

National Aeronautics and Space Administrations. (2015, May 5). Types of Wind Tunnels. Retrieved from <https://www.grc.nasa.gov/www/k-12/airplane/tuntype.html>

Ota, T. (1983), "nose shape effects on turbulence in the separated and reattached flow over blunt flat plates", : Zeitschrift fur Flugwissenschaften und Weltraumforschung, v 7, n 5, p 316-321.

Peter, W., K. (2009), "Fundamentals of Plastics Thermoforming", Morgan & Claypool, PP12-1.

Piancastelli, L., Frizziero, L., Daidzic, N. E., and Rocchi, I. (2013). Analysis of automotive diesel conversions with KERS for future aerospace applications. *International Journal of Heat and Technology*. 31(1): 143-154.

Pope A., Barlow J. B., and Rae W. H. (1999). Low-speed wind tunnel testing. 3rd edition, John Wiley & Sons, Inc.

Rutkay, B., & Laliberté, J. (2016). Design and manufacture of propellers for small unmanned aerial vehicles. *Journal of Unmanned Vehicle Systems*, 4(4), 228-245.
doi:10.1139/juvs-2014-0019

- Shu, X., and Gu, C. (2006), “numerical simulation on the aerodynamic performance of high-speed maglev train with streamlined nose”, Shanghai Jiaotong University Press, China, *Journal of Shanghai Jiaotong University*, v 40, n 6, 1034-7.
- Stathopoulos, T. (1984). Design and fabrication of a wind tunnel for building aerodynamics. *Journal of Wind Engineering and Industrial Aerodynamics*, 16(2-3), 361-376. doi:10.1016/0167-6105(84)90018-7
- Taylor, V. (2014). Qi3 Insight: Unmanned Aerial Vehicles - Growing Markets in a Changing World. Available at: <http://www.qi3.co.uk/wp-content/uploads/2014/02/Qi3-Insights-White-Paper-UAVs-Growing-Markets-in-a-Changing-World-2014021903.pdf>
- Technopedia. (2017). what is an Unmanned Aerial Vehicle (UAV)? - Definition from Techopedia. Retrieved from <https://www.techopedia.com/definition/29896/unmanned-aerial-vehicle-uav>
- D. L. Gabriel, J. Meyer, and F. Du Plessis, “Brushless DC motor characterisation and Selection for a fixed wing UAV,” in Proc. AFRICON, 2011, pp. 1-6.
- Sanchez, et al., “Hovering flight improvement of a quad-rotor mini UAV using brushless DC motors,” *Journal of Intelligent & Robotic Systems*, vol. 61, pp. 85-101, 2011.
- Piancastelli, L., Frizziero, L., Daidzic, N. E., and Rocchi, I. (2013). Analysis of automotive diesel conversions with KERS for future aerospace applications. *International Journal of Heat and Technology*. 31(1): 143-154.

Kumar D, Kannan S and Chand D (2016) “Aerodynamic Analysis of Multi Element Airfoil”

James E. Brunk (2015) “All About Aerodynamics From a Business Card”

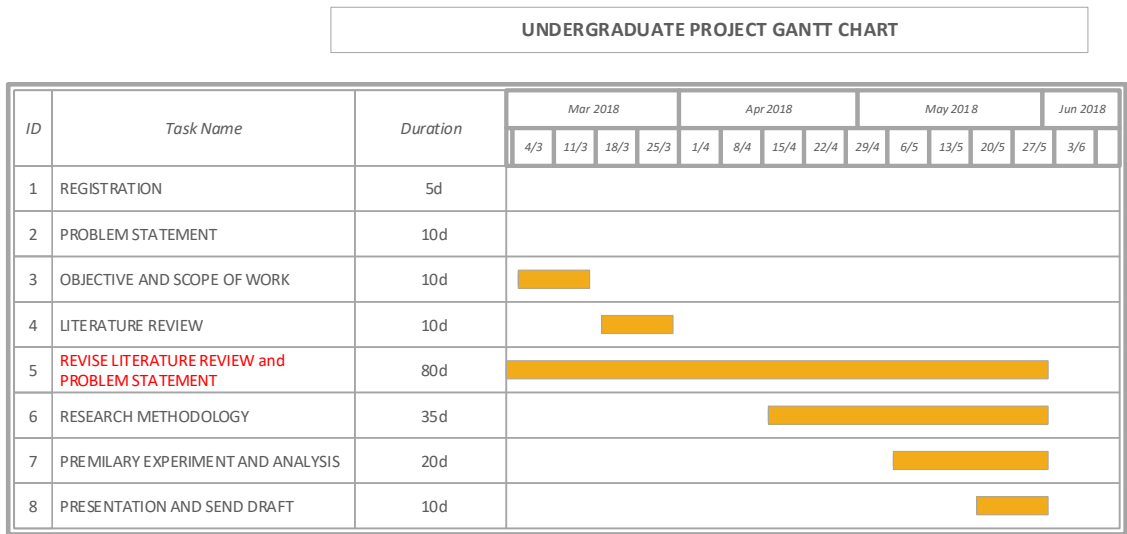
Nur Amalina Musa, Shuhaimi Mansor (2015) “Effect of Tail Dihedral Angle on Lateral Directional Stability due to Sideslip Angles”

Ira H. Abbott, and Albert E. Von Doenhoff (1959)

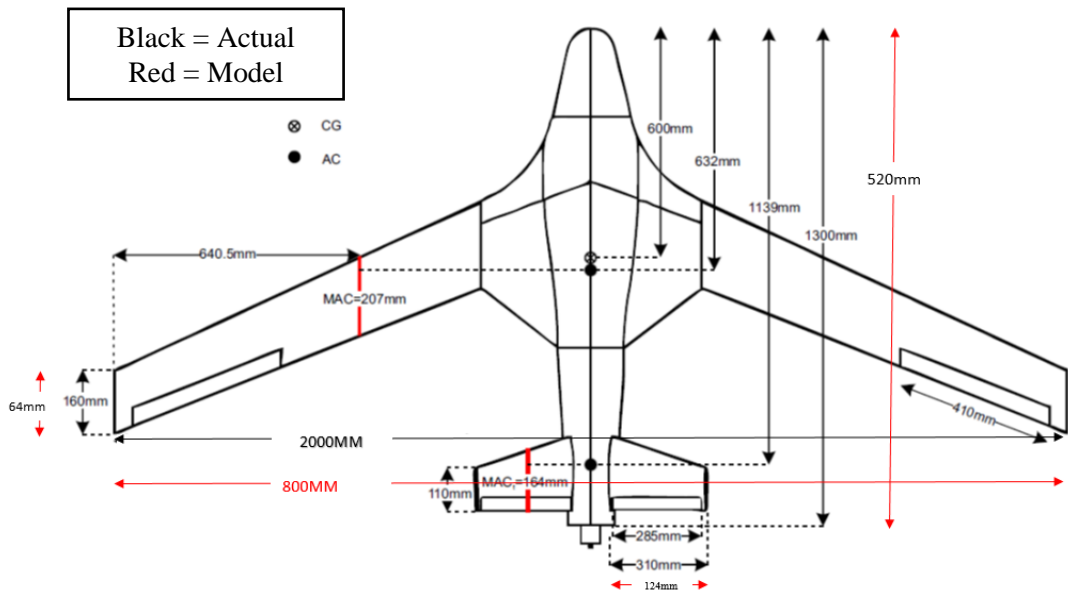
“THEORY OF WING SECTIONS Including a Summary of Airfoil Data”

APPENDICES

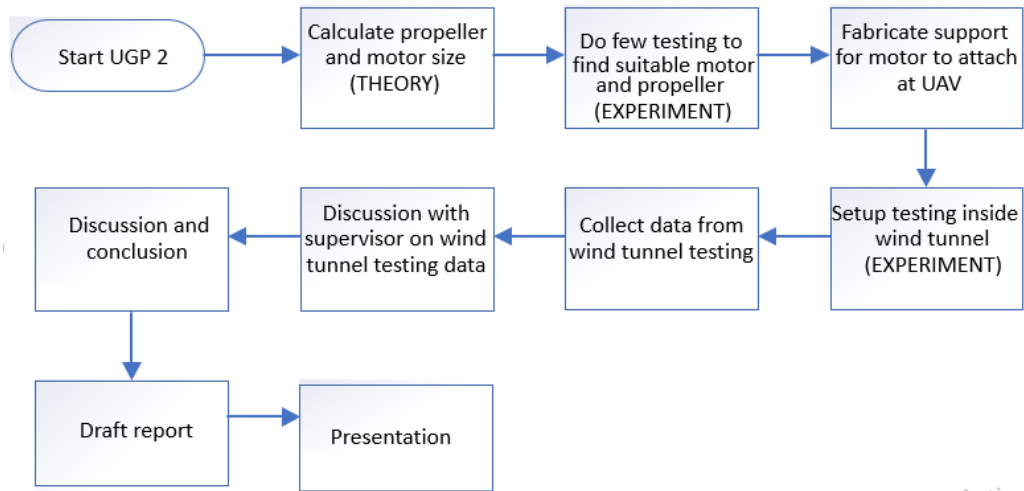
Gantt chart upg1



UAV Dimension



Ugp 2 flow chart



Observation table

Table 3: Observation during wind tunnel testing

PITCH		YAW	
ANGLE	OBSERVATION	ANGLE	OBSERVATION
-4	At 0 rpm motor, 29m/s wind tunnel speed propeller start running itself.	0	0 ampere at 40m/s wind tunnel speed and wing not vibrate
0	Propeller not running.	4	0 ampere at 40m/s wind tunnel speed and wing not vibrate
4	At 0 rpm motor, 33m/s wind tunnel speed propeller start running itself.	8	0 ampere at 40m/s wind tunnel speed and wing not vibrate

8	At 0 rpm motor, 28m/s wind tunnel speed propeller start running itself.	12	wing vibrate at 24m/s and stop vibrate at 36m/s wind tunnel speed
12	Propeller not running.	16	0 ampere at 40m/s wind tunnel speed and wing not vibrate
16	Propeller not running and wing vibrate at wind tunnel speed 26m/s.		

Smoke Testing

